



# Degradation of sunscreen agent 2-phenylbenzimidazole-5-sulfonic acid by TiO<sub>2</sub> photocatalysis: Kinetics, photoproducts and comparison to structurally related compounds

Yuefei Ji<sup>a,b</sup>, Lei Zhou<sup>a</sup>, Corinne Ferronato<sup>b</sup>, Arnaud Salvador<sup>c</sup>, Xi Yang<sup>a,\*</sup>, Jean-Marc Chovelon<sup>b,\*\*</sup>

<sup>a</sup> State Key Laboratory of Pollution Control and Resource Reuse, School of the Environment, Nanjing University, Nanjing 210023, PR China

<sup>b</sup> Université Lyon 1, UMR CNRS 5256, Institut de recherches sur la catalyse et l'environnement de Lyon (IRCELYON), 2 Avenue Albert Einstein, F-69626 Villeurbanne, France

<sup>c</sup> Laboratoire des Sciences Analytiques, Université Lyon 1, UMR 5180, Batiment CPE, 43, Boulevard du 11 novembre 1918, F-69622 Villeurbanne, France

## ARTICLE INFO

### Article history:

Received 12 February 2013

Received in revised form 10 April 2013

Accepted 15 April 2013

Available online 23 April 2013

### Keywords:

Photocatalysis

2-Phenylbenzimidazole-5-sulfonic acid

Hydroxyl radical

Photoproducts

Degradation pathways

## ABSTRACT

The wide occurrence of sunscreen agent micropollutants in natural environment received extensive attention in recent years due to their potential endocrine disrupting effect. The present study focuses on the kinetics and mechanism of photocatalytic degradation of sunscreen agent 2-phenylbenzimidazole-5-sulfonic acid (PBSA) in illuminated TiO<sub>2</sub> suspensions. Photocatalysis of PBSA was systematically investigated under different process conditions and water matrices. Experimental results demonstrated that PBSA photocatalytic reactions followed pseudo-first-order kinetics. Radical scavenging experiments indicated that hydroxyl radical (HO•) is the predominant reactive species responsible for an appreciable degradation of PBSA. Second-order rate constant of PBSA-HO• reaction was determined to be  $5.8 \times 10^9 \text{ M}^{-1} \text{ s}^{-1}$  by competition kinetics method. Major intermediates included hydroxylated products, benzamide, hydroxylated benzimidine, hydroxylated 2-phenyl-1H-benzimidazole as well as phenylimidazolecarboxylic derivatives which were elucidated by means of high performance liquid chromatograph–mass spectrometry (HPLC–MS) technique. Four carboxylic acids, oxalic, malonic, acetic and maleic acids, were detected during PBSA photocatalysis by HPLC–UV analysis. Ion chromatography (IC) results revealed that the sulfonic group of PBSA was primarily converted to sulfate ion while nitrogen atoms were released predominantly as ammonium and to a lesser extent as nitrate. The reduction of TOC processed much more slowly compared to PBSA degradation, however, approximately 80% TOC was removed after 720 min irradiation. A comparison of photocatalytic degradation of PBSA and structurally related compounds revealed that the 5-sulfonic moiety in PBSA had negligible effect on the photocatalysis of 2-phenyl-1H-benzimidazole while 2-phenyl substituent stabilized the benzimidazole ring system to photocatalytic degradation.

© 2013 Elsevier B.V. All rights reserved.

## 1. Introduction

Sunscreens are widely used in personal care products (PCPs) in recent years due to the public awareness of protection against ultraviolet (UV) irradiation and skin cancer [1]. Sunscreens enter the aquatic environment directly as consequence of recreational water activities (e.g., bathing and swimming) or indirectly via wastewater treatment plants (WWTPs) as result of the use of cosmetics, showering, washing, rubbing off and excretion after dermal application

[2,3]. The extensive use of sunscreens already led to frequent detection in many aquatic ecosystems with a considerably high concentration [2–4]. Indeed, sunscreens are regarded as a new kind of environmental contaminants according to the US Environmental Protection Agency [5]. Recent studies have provided evidence that organic sunscreens possess estrogenic properties and behavior as endocrine disrupting chemicals (EDCs) in the environment [6–12]. Furthermore, photo-induced transformation products of some kinds of sunscreens under natural solar irradiation were found to be more toxic than their parent species, which could be a further danger to the biota in environment [9]. Therefore, the long-term and extensive use of sunscreens may cause irreversible adversity on the ecology system.

2-Phenylbenzimidazole-5-sulfonic acid (PBSA), as one kind of sunscreen, is widely used in sunscreen formulations and cosmetics

\* Corresponding author. Tel.: +86 02589680357; fax: +86 02589680357.

\*\* Corresponding author. Tel.: +33 472432638; fax: +33 472448114.

E-mail addresses: [yangxi@nju.edu.cn](mailto:yangxi@nju.edu.cn), [yuefei.ji@ircelyon.univ-lyon1.fr](mailto:yuefei.ji@ircelyon.univ-lyon1.fr) (X. Yang), [jean-marc.chovelon@ircelyon.univ-lyon1.fr](mailto:jean-marc.chovelon@ircelyon.univ-lyon1.fr) (J.-M. Chovelon).

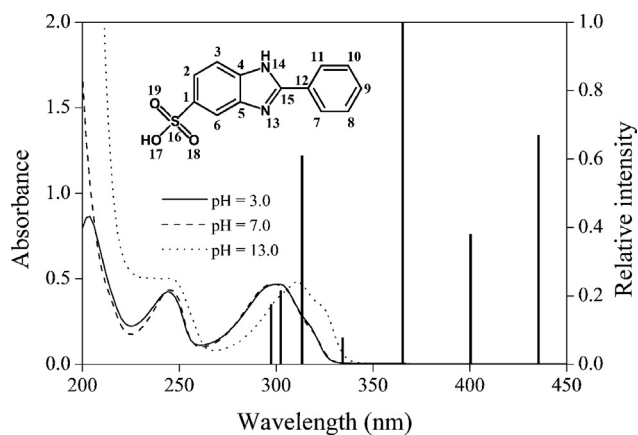


**Fig. 1.** UV-vis absorption spectra of 2-phenylbenzimidazole-5-sulfonic acid (PBSA) at different pH values and emission spectrum of HPK lamp. [PBSA] = 45  $\mu$ M. Note that wavelength with  $\lambda < 340$  nm was filtered by a 340 nm cut-off filter (0–52 Corning) to avoid direct photolysis of PBSA. The insert figure shows the chemical structure of PBSA,  $C_{13}H_{10}O_3N_2S$ . The atoms in PBSA molecular were labeled with numbers for the purpose of frontier electron density (FED) calculation.

because of its strong absorption in the UVB region (see Fig. 1). It has also been approved by the U.S. Food and Drug Administration as an effective sunscreen ingredient based on its ability to prevent erythema [1]. Due to its high polarity and continued input into the environment through personal care applications and incomplete elimination during wastewater treatment, PBSA was frequently detected in natural surface waters with a concentration ranging from 109 to 2679 ng L<sup>-1</sup> [10]. PBSA has been known to photochemically generate reactive oxygen species (i.e.,  $^1O_2$  and  $O_2^{\bullet-}$ ) under UV irradiation and cause DNA damage. For example, Johnson Inbaraj et al. reported that PBSA showed strong oxidizing properties when UV irradiated in neutral aqueous solution in the presence of cysteine, glutathione and azide [13]. Zhang et al. developed a computational method based on the density functional theory (DFT) to predict and evaluate the photodegradation behavior of PBSA and found that energy and electron transfer reactions of excited state PBSA (PBSA\*) could photogenerate  $^1O_2$  and  $O_2^{\bullet-}$  [14,15]. Therefore, it is essential to develop advanced treatment technologies for eliminating PBSA in aqueous solutions for the sake of reducing potential risk to ecological system.

During the past years, various advanced oxidation processes (AOPs) have been reported for the decomposition of organic pollutants in aqueous matrices. Among them, heterogeneous semiconductor photocatalysis using  $TiO_2$  as the photocatalyst has been found to be a promising treatment technology for eliminating organic pollutants, including sunscreens and other PCPs. When irradiating with photons of energy equal to or exceeding the band gap energy of  $TiO_2$  (for anatase, 3.2 eV band gap), valence band holes ( $h_{vb}^+$ ) and reductive conduction band electrons ( $e_{cb}^-$ ) are generated [16,17]. The photogenerated holes can: (i) directly oxidize the adsorbed chemical substance; or (ii) produce adsorbed hydroxyl radical ( $HO^\bullet$ ) via the surface-bound  $OH^-$  and/or the adsorbed water molecules. As a highly reactive oxidant,  $HO^\bullet$  is capable of unselectively reacting with most recalcitrant organic contaminants at near-diffusion-controlled rates in water ( $10^8$ – $10^{10}$  M<sup>-1</sup> s<sup>-1</sup>). Therefore,  $TiO_2$  is considered to be the most suitable semiconductor for widespread environmental photocatalytic applications because it is photoactive, non-toxic, inexpensive, and relatively biologically and chemically stable [16,17].

This study reports on the photocatalytic degradation of PBSA in aqueous suspensions of  $TiO_2$ . The main purpose of this study is to (i) study the influence of process condition and water matrix on photocatalytic degradation; (ii) clarify the dominant reactive species

involved in photocatalysis process; (iii) characterize intermediates and photoproducts; (iv) elucidate the mechanism and transformation pathways leading to PBSA mineralization; (v) compare with structurally related compounds in photocatalytic degradation. To the authors' knowledge, this is the first study that includes a systematic exploration of kinetics, intermediates and degradation pathways of PBSA photocatalytic degradation.

## 2. Experimental

### 2.1. Chemicals and materials

PBSA, 2-phenyl-1H-benzimidazole and benzimidazole were purchased from Sigma-Aldrich and used as received. Commercial humic acid (sodium salt) was purchased from Aldrich. HPLC grade methanol and acetonitrile were obtained from Fisher Scientific. Other reagents were at least of analytical grade and used as received without further purification. Non-porous titanium dioxide (Degussa P25  $TiO_2$ , Germany) with primary particle diameter of 30 nm, specific surface area of 50 m<sup>2</sup> g<sup>-1</sup> and crystal distribution of 80% anatase and 20% rutile was used as the photocatalyst for most of the experiments. Hombikat UV100 (100% anatase, 5 nm, 250 m<sup>2</sup> g<sup>-1</sup>) and Aldrich rutile (100% rutile, 750 nm, 3 m<sup>2</sup> g<sup>-1</sup>) were also used as photocatalysts in the preliminary experiment. Syringes (Injekt-F, 1 mL) were purchased from B. Braun. Millex-HV syringe filters (PVDF, 0.45  $\mu$ m) were purchased from Millipore Corporation. All the solutions were prepared with 18 M $\Omega$  cm water from a Milli-Q water purification system.

### 2.2. Photocatalysis procedures

The photocatalytic experiments were performed in an open Pyrex glass cell with approximately 60 mL volume containing the aqueous suspension of  $TiO_2$  powder and PBSA. The irradiation source was a high pressure mercury lamp (HPK 125W, Heraeus) with maximum emission wavelength mainly around 365 nm. Infrared radiation (IR) was well filtered by water circulation in the reactor jacket which maintained the temperature at  $20 \pm 1^\circ$ C. Direct photolysis caused by UV irradiation was avoided by using a 340 nm cut-off filter (0–52 Corning). The radiant flux entering the reactor was measured directly by a VLX-3W radiometer with a CX-365 detector (UV-A) and was found to be approximately 3.32 mW cm<sup>-2</sup>. A volume of 25 mL aqueous solution containing PBSA and  $TiO_2$  powder with required concentration was introduced in the reactor. Before irradiation, the suspension was magnetically stirred in the dark for 30 min to reach adsorption-desorption equilibrium. During irradiation, aliquots of samples ( $\sim 300$   $\mu$ L) were withdrawn with the help of syringe at various intervals and filtered through syringe filters to remove  $TiO_2$  particles before analysis. The adsorption of PBSA on filters was found to be negligible based on a preliminary test. Total volume of the samples withdrawn from each experiment was less than 10% (by volume) of the reaction solution. The pH of the reaction solution was adjusted by adding 0.1 M  $HClO_4$  or 0.1 M NaOH.

### 2.3. Analytical procedures

A Shimadzu 10A series high performance liquid chromatography (Shimadzu, Japan) with a SPD-M10A DAD was employed to analyze the concentration of PBSA, 2-phenyl-1H-benzimidazole, benzimidazole and benzoic acid, as well as the abundance of the photocatalytic degradation intermediates. The intermediates generated during photocatalysis of PBSA were analyzed by a HP 1100 series HPLC system equipped with a API 3000 triple quadrupole mass spectrometer (Applied Biosystems/MDS Analytical Technologies, Foster City, CA, USA) and coupled with a TurbolonSpray source

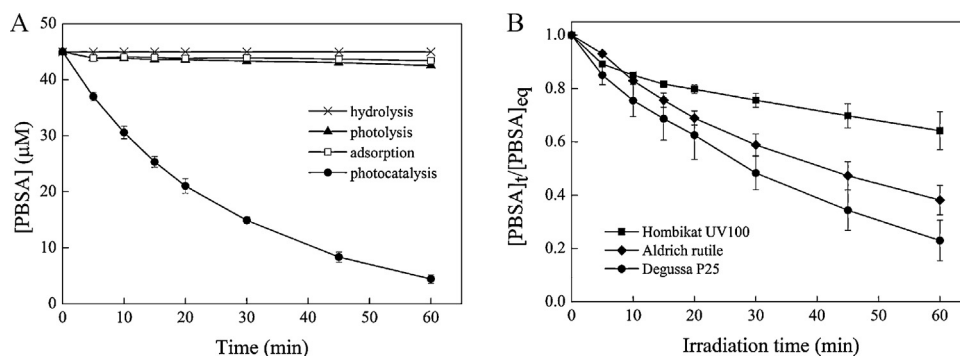


**Fig. 2.** (A) Comparison of hydrolysis, photolysis, adsorption and photocatalysis of PBSA in aqueous solutions. Degussa P25 TiO<sub>2</sub> was used as photocatalyst. [TiO<sub>2</sub>] = 1.0 g L<sup>-1</sup>; [PBSA] = 45 μM; pH = 7.0. (B) Effect of different photocatalysts on PBSA photocatalytic degradation. [TiO<sub>2</sub>] = 1.0 g L<sup>-1</sup>; [PBSA] = 45 μM; pH = 4.5. Error bars represent 95% confidence intervals.

(TIS) operated in positive ion mode for the MS measurements. The detection of carboxylic acids was performed using a HPLC–UV system (Varian 9010 model) equipped with a ICsep-GOREGEL-87H3 cation exchange column (9 μm, 300 mm × 7.8 mm, i.d.) (Transgenomic, USA). The analyses of inorganic ions released during photocatalysis process were carried out by using a Metrohm ion chromatographic instrument (881 Compact IC Pro, Switzerland). To determine the extent of mineralization during photocatalysis, total organic carbon (TOC) of filtered suspension samples was measured using a TOC-5050A analyzer (Shimadzu). The UV–vis absorption spectra of PBSA and humic acid aqueous solutions were recorded using a Lambda 950 UV–vis spectrophotometer (PerkinElmer, USA) equipped with quartz cuvettes (optical path length 1.0 cm). The pH of the solutions was measured with a combined glass electrode connected to a PHM 210 standard pH meter (Radiometer, Copenhagen, Denmark). The analytical details are presented in the Supplementary Data.

#### 2.4. Determination of second-order rate constant of PBSA-HO• reaction

The second-order rate constant for reaction of PBSA with HO• was determined by competition kinetics method using Fenton's reagent as HO• generation source [18]. The detailed procedure is shown in the Supplementary Data.

#### 2.5. Calculation of frontier electron density of PBSA

Molecular orbital calculations were carried out at the single determinant (B3LYP/6-311+G\*) level with the optimal conformation having a minimum energy obtained at the same level in a Gaussian 09 program. The frontier electron densities (FEDs) of the highest occupied molecular orbital (HOMO) and the lowest unoccupied molecular orbital (LUMO) were determined. Values of  $FED_{HOMO}^2 + FED_{LUMO}^2$  were calculated to predict the reaction sites for hydroxyl addition.

### 3. Results and discussion

#### 3.1. Preliminary experiments of PBSA photocatalytic degradation

Preliminary experiments of hydrolysis (without TiO<sub>2</sub> in dark), direct photolysis (without TiO<sub>2</sub> under irradiation) and adsorption (with TiO<sub>2</sub> in dark) were carried out to assess their contribution to photocatalytic degradation of PBSA by Degussa P25 TiO<sub>2</sub> as presented in Fig. 2A. As seen, no loss of PBSA was observed due to hydrolysis, suggesting PBSA was stable in Milli-Q water under dark condition. Dark controls also indicated that PBSA was stable in aqueous solution with pH ranging from 3 to 13 without light.

Direct photolysis of PBSA in Milli-Q water contributed to a negligible degradation of PBSA (less than 5%), which can be attributed to an unappreciable overlap of PBSA UV–vis absorption spectrum ( $\lambda < 340$  nm) and the emitting spectrum (340–800 nm) of the filtered HPK lamp used as irradiation source in our study (see Fig. 1). Adsorption of PBSA on TiO<sub>2</sub> was also found to be marginal probably due to the relatively high hydrophilicity of PBSA (solubility 0.26 g L<sup>-1</sup>). Therefore, hydrolysis, direct photolysis and adsorption contributed insignificantly to the decay of PBSA in comparison to photocatalysis.

In order to choose the most suitable catalyst for PBSA photocatalytic degradation, experiments using different kinds of catalysts (i.e., Degussa P25, Aldrich rutile and Hombikat UV100) were carried out (Fig. 2B). As seen, photocatalytic degradation of PBSA proceeded much more rapidly in the presence of P25 relative to other photocatalysts. The photoreactivities of these catalysts followed the order Degussa P25 > Aldrich rutile > Hombikat UV100. The substantially higher activity of P25 is not unexpected, since similar results were observed by other authors [19,20]. The low re-combination rate of photogenerated electrons and holes due to a mixture crystal structure of P25 compared to other pure crystal catalyst is believed to be responsible for a significantly higher photoactivity [20]. However, it should be noted that the photocatalytic activity of TiO<sub>2</sub> depends on various parameters in a complex way (e.g., crystallinity, surface, particle size, defect sites, surface charge) [21]. Recent studies also have shown that the photocatalytic activity of TiO<sub>2</sub> is highly substrate-specific [22]. Concerning the preliminary experiment result, our subsequent runs were carried out using P25 as photocatalyst.

#### 3.2. Determination of major reactive species

Preliminary experiment demonstrated that TiO<sub>2</sub> mediated photocatalysis was responsible for an appreciable degradation of PBSA. During photocatalysis process, photo-excited separation of valence band holes ( $h_{vb}^+$ ) and reductive conduction band electrons ( $e_{cb}^-$ ) occur when TiO<sub>2</sub> absorbs photons with energy larger than band gap. The highly oxidative  $h_{vb}^+$  can be transferred to the surface-adsorbed water or hydroxyl groups (i.e., titanol group) to form the surface-bound hydroxyl radical ( $HO^{\bullet}_{surf}$ ) or free hydroxyl radical ( $HO^{\bullet}_{free}$ ) after desorption from the surface. On the other hand,  $e_{cb}^-$  transfers to dissolved oxygen, leading to the production of superoxide radical anion ( $O_2^{\bullet-}$ ) and hydroperoxyl radical ( $HO_2^{\bullet}$ ) and its further reduction to hydrogen peroxide ( $H_2O_2$ ) [23–25]. Among them, HO• (either adsorbed or free) is often assumed to be the major species responsible for the photocatalytic oxidation, based on the evidences including detection of hydroxylated intermediates, distribution of the hydroxylation products, and spin trapping with subsequent ESR detection [24]. On the other hand,

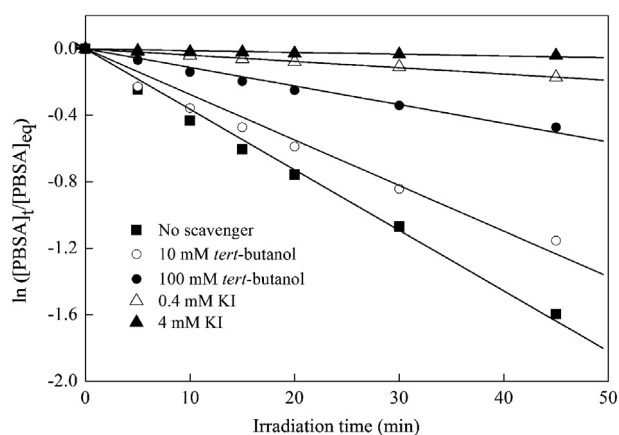


**Fig. 3.** Effect of radical scavengers on PBSA photocatalytic degradation. The *tert*-butanol was used as a scavenger of  $\text{HO}^\bullet$  while KI was used as a scavenger of both  $h_{\text{vb}}^+$  and  $\text{HO}^\bullet$ . Experimental conditions: Degussa P25  $\text{TiO}_2$  was used as photocatalyst;  $[\text{TiO}_2] = 2.0 \text{ g L}^{-1}$ ;  $[\text{PBSA}] = 37.9 \mu\text{M}$ ;  $\text{pH} = 4.5$ .

direct hole oxidation through electron transfer is also feasible since the oxidation potentials of most organic compounds lie below that of  $h_{\text{vb}}^+$ . For example, carboxylic acids, lacking abstractable hydrogens or C–C unsaturation, are believed to be oxidized primarily by  $h_{\text{vb}}^+$  via a photo-Kolbe process [26].

In order to verify the photocatalysis mechanism and distinguish the contribution of these reactive species, radical scavengers are usually employed as diagnostic tools to investigate the importance of certain kind of radicals since these scavengers selectively react with radicals to form stable or persistent intermediates [26–29]. For example, alcohols such as isopropanol, methanol and *tert*-butanol, have been commonly used to estimate  $\text{HO}^\bullet$  mediated mechanism [26,27]. The direct oxidation of these alcohols by  $h_{\text{vb}}^+$  is believed to be negligible because they have a very low affinity to  $\text{TiO}_2$  surface in aqueous solution [27]. Iodide ion is an excellent scavenger that reacts with  $h_{\text{vb}}^+$  and adsorbed  $\text{HO}^\bullet$  because  $h_{\text{vb}}^+$  can be easily captured by  $\text{I}^-$  (an electron donor) and oxidation of  $\text{I}^-$  by surficial  $\text{HO}^\bullet$  is also possible [28,29].

In this study, *tert*-butanol, as a scavenger of  $\text{HO}^\bullet$  ( $5.0 \times 10^8 \text{ M}^{-1} \text{ s}^{-1}$ ) [23], and potassium iodide (KI), as a scavenger of both  $h_{\text{vb}}^+$  and  $\text{HO}^\bullet$  ( $1.2 \times 10^{10} \text{ M}^{-1} \text{ s}^{-1}$ ) [28] were used and the results are shown in Fig. 3. It was observed that PBSA photocatalysis reactions with or without radical scavengers all followed pseudo-first-order kinetics. The obtained pseudo-first-order rate constants as well as corresponding linear correlation coefficient are presented in Table S2 (Supplementary Data).

In Fig. 3, the control run (no scavenger) exhibited a degradation rate constant of  $0.0486 \text{ min}^{-1}$ , resulting from combined effects of all the possible radicals. However, the degradation rate constant decreased more than 92% and 97% in the presence of 0.4 mM and 4 mM KI, respectively. This suggests that both  $\text{HO}^\bullet$  and  $h_{\text{vb}}^+$  together were responsible for the major degradation of PBSA, while other radicals such as  $\text{O}_2^{\bullet-}$ ,  $\text{HO}_2^\bullet$  and  $\text{H}_2\text{O}_2$  contributed insignificantly to PBSA degradation. To determine the relative contribution between  $\text{HO}^\bullet$  and  $h_{\text{vb}}^+$ , further runs using *tert*-butanol as  $\text{HO}^\bullet$  scavenger were carried out. In Fig. 3, the addition of 10 mM and 100 mM *tert*-butanol resulted in a degradation rate constant of  $0.0274 \text{ min}^{-1}$  and  $0.0112 \text{ min}^{-1}$ , respectively, which decreased by 43% and 77% compared with control run. Hence,  $\text{HO}^\bullet$  was likely to be the most important radical during PBSA photocatalytic degradation. It is believed that reaction with holes is more important for hydrophobic compounds that are repelled from the aqueous solution and are thus more likely to undergo adsorption on the photocatalyst surface [22]. Therefore, the relatively higher hydrophilicity of PBSA and lower adsorption may be one reason accounting for the less

importance of  $h_{\text{vb}}^+$ . Since  $\text{HO}^\bullet$  is highly electrophilic, we speculate that the rich  $\pi$  electron system of benzimidazole and phenyl moiety of PBSA molecular favor  $\text{HO}^\bullet$  attack, which in turn enables  $\text{HO}^\bullet$  playing a more important role than other radicals. This hypothesis is further verified by the intermediates that were identified by LC–MS.

Second-order rate constant of PBSA– $\text{HO}^\bullet$  reaction was determined by competition kinetic method as described in Section 2 according to the following equation [29].

$$\ln \left( \frac{[\text{PBSA}]_t}{[\text{PBSA}]_0} \right) = \frac{k_{\text{HO}^\bullet, \text{PBSA}}}{k_{\text{HO}^\bullet, \text{BA}}} \ln \left( \frac{[\text{BA}]_t}{[\text{BA}]_0} \right) \quad (1)$$

where BA is the reference compound, benzoic acid, with a known rate constant of reaction with  $\text{HO}^\bullet$  ( $k_{\text{HO}^\bullet, \text{BA}} = 5.9 \times 10^9 \text{ M}^{-1} \text{ s}^{-1}$ ) [29]. From Eq. (1), the second-order rate constant of PBSA– $\text{HO}^\bullet$  reaction was calculated to be  $5.8 \times 10^9 \text{ M}^{-1} \text{ s}^{-1}$  by plotting of  $\ln([\text{PBSA}]_t/[\text{PBSA}]_0)$  versus  $\ln([\text{BA}]_t/[\text{BA}]_0)$  (see Fig. S1, Supplementary Data). Such a high second order rate constant suggests that PBSA could readily react with  $\text{HO}^\bullet$  near the diffusion-controlled limit. This observation further supports the result of radical scavenging experiment, that,  $\text{HO}^\bullet$  is the most important radical involved in PBSA photocatalysis.

### 3.3. Effect of process conditions and water matrices on PBSA photocatalytic degradation

Further batch experiments under different process conditions (i.e., catalyst loading, initial substrate concentration and solution pH) were performed for the purpose of a systematic study and the obtained overall results are summarized in Table 1. Our results reveal that photocatalytic degradation of PBSA under different operation conditions followed pseudo-first-order kinetics.

For the  $\text{TiO}_2$  loading, the initial reaction rate  $r_0$ , which was calculated over the course of first 5 min of irradiation, increased with increasing catalyst loading up to a certain value, while further increasing the catalyst loading significantly reduced  $r_0$  (Table 1). It is proposed that with  $\text{TiO}_2$  dosage increasing, more photons are expected to be absorbed by  $\text{TiO}_2$ , which consequently leads to higher amount of reactive species [17]. The enhanced concentrations of reactive species are generally responsible for a much faster degradation. However, when  $\text{TiO}_2$  loading was higher than  $2.0 \text{ g L}^{-1}$ , a decreased  $r_0$  was observed which can be explained by screening effect of excess particles, masking part of the photo-sensitive surface, as well as scattering or reflecting the amount of photons needed for exciting the catalyst [30,31]. In addition, a higher  $\text{TiO}_2$  loading usually leads to aggregation of the photocatalyst particles that decreases the contact surface area between reactant and photocatalyst, and consequently, reduces the number of active sites and lowers the rate of photodegradation [32].

Previous studies have reported the dependency of the  $\text{TiO}_2$  photocatalytic reaction rate on the concentration of the organic substrate [20,30,31]. Table 1 also illustrates the effect of different initial concentration of PBSA on the initial reaction rate  $r_0$ . As seen,  $r_0$  increased as the concentration of PBSA increased up to a maximum value, while further elevating the concentration led to a decreased reaction rate. The enhancement of  $r_0$  with increasing PBSA concentration could be explained by the scavenging of reactive species by the substrate. The reaction of PBSA with  $\text{HO}^\bullet$  and  $h_{\text{vb}}^+$  on the surface of  $\text{TiO}_2$  is in competition with the thermal recombination process  $\text{HO}^\bullet/\text{e}_{\text{cb}}^-$  and  $h_{\text{vb}}^+/\text{e}_{\text{cb}}^-$ . An excessive concentration of PBSA could completely inhibit the unfavorable recombination, thus, the initial reaction rate of PBSA can be expected to reach a maximum value equivalent to the trapping rate of  $\text{HO}^\bullet$  and  $h_{\text{vb}}^+$  on  $\text{TiO}_2$  surface. During photocatalysis process, organic compounds generally transform to radical transient at the first step by reacting with  $h_{\text{vb}}^+$  and  $\text{HO}^\bullet$  (e.g.,  $\text{HO}^\bullet$  adduct or



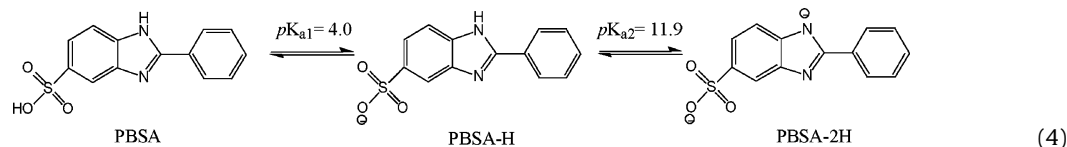
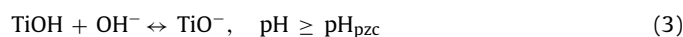
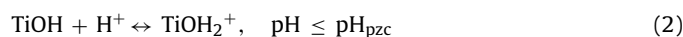
**Table 1**Results of batch experiments for degradation of PBSA by TiO<sub>2</sub> photocatalysis.

Photocatalyst	TiO <sub>2</sub> (g L <sup>-1</sup> )	C <sub>0</sub> (μM) <sup>a</sup>	pH <sup>b</sup>	HCO <sub>3</sub> <sup>-</sup> (mM)	HA <sup>c</sup> (mg L <sup>-1</sup> )	k <sub>p</sub> (min <sup>-1</sup> ) <sup>d</sup>	r <sub>0</sub> (μM min <sup>-1</sup> ) <sup>e</sup>	R <sup>2</sup> <sup>f</sup>
1. Effect of photocatalyst type								
Aldrich rutile	1.0	45	4.5	0	0	0.0184	–	0.999
Hombikat UV100	1.0	45	4.5	0	0	0.0095	–	0.969
Degussa P25	1.0	45	4.5	0	0	0.0285	–	0.998
2. Effect of photocatalyst loading								
Degussa P25	0.25	37.9	4.5	0	0	–	1.14	–
Degussa P25	0.5	37.9	4.5	0	0	–	1.47	–
Degussa P25	1.0	37.9	4.5	0	0	–	1.61	–
Degussa P25	1.5	37.9	4.5	0	0	–	2.20	–
Degussa P25	2.0	37.9	4.5	0	0	–	2.36	–
Degussa P25	3.0	37.9	4.5	0	0	–	0.94	–
3. Effect of substrate concentration								
Degussa P25	2.0	8.85	4.5	0	0	–	1.57	–
Degussa P25	2.0	22.1	4.5	0	0	–	1.63	–
Degussa P25	2.0	37.9	4.5	0	0	–	2.36	–
Degussa P25	2.0	44.3	4.5	0	0	–	2.06	–
Degussa P25	2.0	61.7	4.5	0	0	–	1.54	–
4. Effect of solution pH								
Degussa P25	2.0	37.9	2.5	0	0	0.0203	–	0.998
Degussa P25	2.0	37.9	4.5	0	0	0.0486	–	0.991
Degussa P25	2.0	37.9	8.5	0	0	0.0521	–	0.999
Degussa P25	2.0	37.9	10.9	0	0	0.0466	–	0.999
Degussa P25	2.0	37.9	11.3	0	0	0.0163	–	0.997
5. Effect of bicarbonate ion								
Degussa P25	2.0	37.9	8.5	1	0	0.0383	–	0.999
Degussa P25	2.0	37.9	8.5	10	0	0.0310	–	0.999
Degussa P25	2.0	37.9	8.5	100	0	0.0062	–	0.999
6. Effect of humic acid								
Degussa P25	2.0	37.9	5.5	0	6	0.0417	–	0.990
Degussa P25	2.0	37.9	5.5	0	18	0.0220	–	0.999
Degussa P25	2.0	37.9	5.5	0	60	0.0028	–	0.931

<sup>a</sup> The initial concentration of PBSA.<sup>b</sup> The pH of the solutions was adjusted by 0.1 M HClO<sub>4</sub> or 0.1 M NaOH.<sup>c</sup> HA represents humic acid.<sup>d</sup> k<sub>p</sub> is the pseudo-first-order rate constant.<sup>e</sup> r<sub>0</sub> is the initial reaction rate which was calculated from the slope value of PBSA degradation curve over the first 5 min of reaction. r<sub>0</sub> was calculated instead of k<sub>p</sub> for investigating the effect of catalyst loading and initial organic substrate on photodegradation efficiency.<sup>f</sup> R<sup>2</sup> is the linear correlation coefficient.

H-abstract). These partially oxidized radical transient could either undergo further oxidation to a non-radical stable intermediate or react with an electron to return back to the initial substrate. The so-called back or recombination reaction will become dominant when the substrate concentration is high enough, which negatively contributes to a decreased initial reaction rate [33]. Considering

and PBSA in different pH solutions is according to the following equations.



the elevated initial concentration of PBSA, a larger yield amount of intermediates can also be expected, which are capable of poisoning the TiO<sub>2</sub> active sites and/or competing for photons with the catalyst, leading to a decreased transformation rate of mother compound [33].

The effect of solution pH on photocatalytic degradation is a complex issue related to the ionization states of organic compounds and the surface charge of catalyst as well as the formation rate of HO• and other active radicals in the reaction solution [17,30]. The solution pH also alters the TiO<sub>2</sub> energy levels according to the Nernstian behavior (−59 mV/pH) due to the pH-dependent surface charge [25]. Since the point of zero charge (pH<sub>pzc</sub>) of Degussa P25 is widely reported to be 6.25 and PBSA has two pK<sub>a</sub> (i.e., pK<sub>a1</sub> = 4.0 and pK<sub>a2</sub> = 11.9) due to the presence of sulfonic and imidazole moiety in PBSA molecular [13], the predominant existing speciation of TiO<sub>2</sub>

As shown in Table 1, photocatalytic degradation of PBSA is highly pH-dependent. At pH 2.5, the relatively low photodegradation rate constant was most likely due to the lack of electrostatic attraction between TiOH<sub>2</sub><sup>+</sup> and PBSA. Accordingly, the comparatively high rate constant at pH 4.5 can be attributed to the electrostatic attraction between TiOH<sub>2</sub><sup>+</sup> and PBSA-H, which facilitates the adsorption of PBSA on TiO<sub>2</sub> surface. However, the high rate constant at pH 8.5 was unexpected since electrostatic repulsion was expected to take place between TiO<sup>−</sup> and PBSA-H. Therefore, the pH-dependent effect of HO• formation rate was likely responsible for such phenomenon because previous literatures have demonstrated that alkaline condition could promote photogeneration of hydroxyl radicals [19,34,35]. Nevertheless, at extremely high pH (pH = 13.0), the electrostatic repulsion between TiO<sup>−</sup> and PBSA-2H would become much stronger, which out-competed the positive effect of HO• formation, and consequently decreased the degradation rate constant.

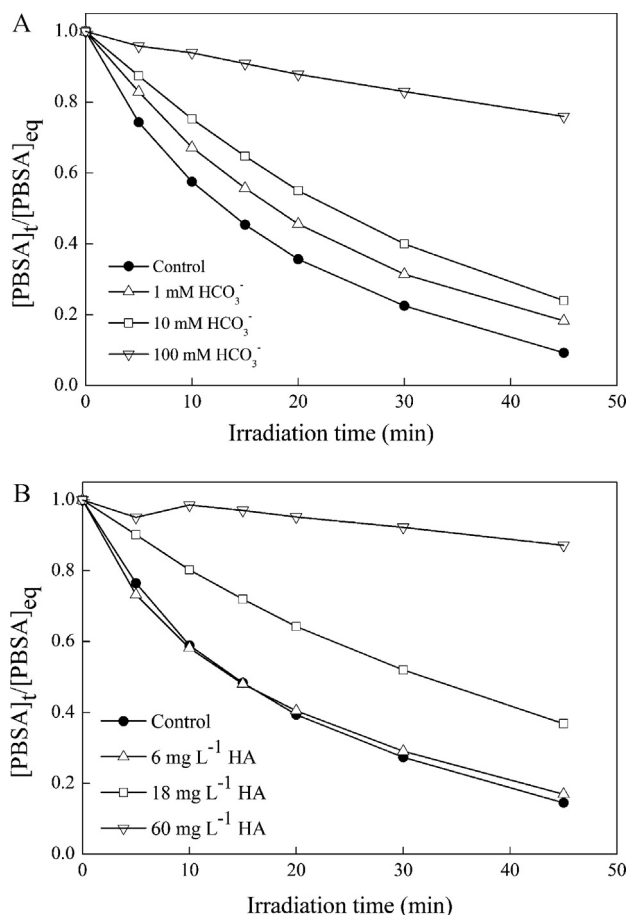
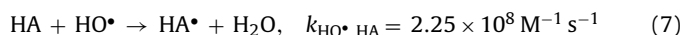
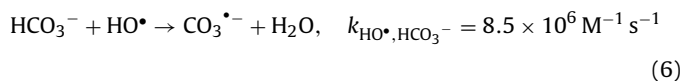
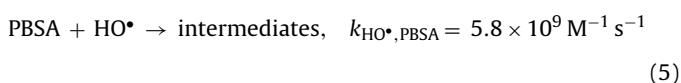


**Fig. 4.** Effect of (A) bicarbonate ion (pH=8.5), and (B) humic acid (pH=5.5) on PBSA photocatalytic degradation. Experimental conditions: Degussa P25  $\text{TiO}_2$  was used as photocatalyst;  $[\text{TiO}_2] = 2.0 \text{ g L}^{-1}$ ;  $[\text{PBSA}] = 37.9 \mu\text{M}$ ;  $[\text{HCO}_3^-] = 0\text{--}100 \text{ mM}$ ;  $[\text{HA}] = 0\text{--}60 \text{ mg L}^{-1}$ .

Water matrix plays an important role in photocatalytic degradation of organic compounds because some constituents that are ubiquitous in natural waters (e.g., bicarbonate ions, dissolved organic matter (DOM)) may serve as  $\text{HO}^\bullet$  scavengers [36,37]. From this viewpoint, bicarbonate ( $\text{HCO}_3^-$ ) and humic acid (HA) were chosen to investigate their effect on the photocatalysis degradation of PBSA since they are not only well-known  $\text{HO}^\bullet$  scavengers but are also widely present in natural waters. Experiments were conducted in aqueous  $37.9 \mu\text{M}$  PBSA solutions with a  $\text{HCO}_3^-$  concentration range of 0–100 mM or a HA concentration range of 0–60  $\text{mg L}^{-1}$ . Note that, in the case of  $\text{HCO}_3^-$ , solution pH was maintained at 8.5 to ensure  $\text{HCO}_3^-$  was the dominant species ( $\text{pK}_{\text{a}1} = 6.37$  and  $\text{pK}_{\text{a}2} = 10.25$ ) in the reaction solution.

It is evident that the presence of  $\text{HCO}_3^-$  or HA suppressed the photocatalytic degradation of PBSA (Table 1 and Fig. 4). For example, PBSA transformation ratio was found to be only 24% and 12.2% after 45 min irradiation in the presence of 100 mM  $\text{HCO}_3^-$  or 60  $\text{mg L}^{-1}$  HA, respectively, compared to 92.4% and 85.5% in absence of  $\text{HCO}_3^-$  (pH=8.5) or HA (pH=5.5), respectively. The inhibition can be ascribed to the competition for  $\text{HO}^\bullet$  by  $\text{HCO}_3^-$  and HA. It is assumed that if the PBSA coexists with  $\text{HCO}_3^-$  or HA in reaction solution, the  $\text{HO}^\bullet$  will be partitioned according to the following equations [38,39].



Therefore, a fraction of  $\text{HO}^\bullet$  will be quenched by  $\text{HCO}_3^-$  or HA. If we assume that  $\text{HO}^\bullet$  yield amount remained constant during photocatalysis, the increase in the concentration of  $\text{HCO}_3^-$  or HA would lower the amount of  $\text{HO}^\bullet$ , leading less  $\text{HO}^\bullet$  available for reacting with PBSA. For HA at higher concentration, competitive adsorption on  $\text{TiO}_2$  active sites and light attenuating may also occur simultaneously (see Fig. S2, the adsorption mass ( $\text{mg/g TiO}_2$ ) of HA on  $\text{TiO}_2$  versus time and Fig. S3, the UV–vis absorption spectra of HA at different concentration, Supplementary Data) [40]. These factors may together retard PBSA photocatalytic degradation. Nevertheless, at lower concentration (e.g., 1 mM  $\text{HCO}_3^-$  or 6  $\text{mg L}^{-1}$  HA), the presence of  $\text{HCO}_3^-$  or HA showed slight inhibition on PBSA photocatalysis. Since the environmentally relevant concentration of  $\text{HCO}_3^-$  and HA are reported to be 0.4–4 mM and 0.3–30  $\text{mg L}^{-1}$ , respectively [38,41], this observation is particularly interesting because of the feasibility of applying  $\text{TiO}_2$  photocatalysis for treating PBSA micropollutant in environmentally realistic water matrix. It is worth noting that quenching of  $\text{HO}^\bullet$  by  $\text{HCO}_3^-$  yields carbonate radical ( $\text{CO}_3^{\bullet-}$ ) (Eq. (6)), and  $\text{CO}_3^{\bullet-}$  may react with PBSA due to its electron rich nature. However, no enhancement in photocatalytic degradation of PBSA was observed in this study as the  $\text{HCO}_3^-$  concentration increased. Given that  $\text{CO}_3^{\bullet-}$  is generally less reactive than  $\text{HO}^\bullet$  (second-order rate constant for reaction of  $\text{CO}_3^{\bullet-}$  with organic compound is normally 2–3 magnitude order lower than that of  $\text{HO}^\bullet$ ) [38,39], it is possible that  $\text{CO}_3^{\bullet-}$ -mediated PBSA oxidation was negligible in the present study.

### 3.4. Identification of photodegradation intermediates and products

#### 3.4.1. Evolution of organic intermediates

Advanced oxidation processes often yield various degradation intermediates and products due to the non-selective reaction of  $\text{HO}^\bullet$  with organic pollutants. In this work, we have attempted to identify photodegradation intermediates using LC–MS technique. A mixture sample composed of aliquots withdrawn at different irradiation time was analyzed for the purpose of identifying as more intermediates as possible. Structural identification of these intermediates was based on the analysis of the total ion chromatogram (TIC) and the corresponding mass spectrum (Fig. S4 and Table S3, Supplementary Data). Major intermediates included hydroxylation products (mono-, di- and tri-hydroxylated PBSA), imidazole ring cleavage products (e.g., benzamide), and hydroxylated 2-phenyl-1H-benzimidazole as well as phenylimidazolecarboxylic derivatives.

In order to correctly characterize mono-hydroxylated compounds (positions of hydroxylation), the frontier electron densities (FEDs) of PBSA (as PBSA-H form) were calculated to predict the reaction sites for  $\text{HO}^\bullet$  attacking, and the obtained results are summarized in Table 2. In the Frontier Orbital Theory, the preferential  $\text{HO}^\bullet$  addition probably takes place on the atom with the highest  $\text{FED}_{\text{HOMO}}^2 + \text{FED}_{\text{LUMO}}^2$  value [42,43], which has been proved to be reasonable by the published work [44]. As shown in Table 2, 9C, 11C, 7C and 8C sites in phenyl ring and 2C in benzimidazole have the highest  $\text{FED}_{\text{HOMO}}^2 + \text{FED}_{\text{LUMO}}^2$  value, implying both the two benzenes are likely to be attacked by  $\text{HO}^\bullet$ , resulting in the formation of mono-hydroxylation products. However, it should be noted that the possibility for  $\text{HO}^\bullet$  addition to phenyl moiety is much higher than addition to benzyl moiety which is adjacent to imidazole.

**Table 2**

FED<sub>HOMO</sub><sup>2</sup> + FED<sub>LUMO</sub><sup>2</sup> values of PBSA (PBSA-H form) atoms calculated by using Gaussian 09 program at the B3LYP/6-311+G\* level.

Number (atom) <sup>a</sup>	FED <sub>HOMO</sub> <sup>2</sup> + FED <sub>LUMO</sub> <sup>2</sup>	Number (atom)	FED <sub>HOMO</sub> <sup>2</sup> + FED <sub>LUMO</sub> <sup>2</sup>
1C	0.0054	<b>11C</b>	<b>0.0927</b>
<b>2C<sup>b</sup></b>	<b>0.0339</b>	12C	0.1916
3C	0.0151	13N	0.0722
4C	0.0130	14N	0.0451
5C	0.0021	15C	0.0438
6C	0.0280	16S	0.0001
<b>7C</b>	<b>0.0701</b>	17O	0.1793
<b>8C</b>	<b>0.0474</b>	18O	0.1996
<b>9C</b>	<b>0.2112</b>	19O	0.1877
10C	0.0306		

<sup>a</sup> See Fig. 1 for atom numbering.

<sup>b</sup> Atoms in bold means these atoms have the highest FED<sub>HOMO</sub><sup>2</sup> + FED<sub>LUMO</sub><sup>2</sup> values, thus are more likely to be attacked by hydroxyl radical.

Although the 12C has a much higher FED<sub>HOMO</sub><sup>2</sup> + FED<sub>LUMO</sub><sup>2</sup> value, we speculate that it is unlikely that the HO• will attack this site due to steric hindrance.

Fig. 5A describes the evolution profiles of five major intermediates of PBSA (i.e., mono-hydroxylated benzimidine (OH-BZMD); three isomers of mono-hydroxylated PBSA (OH-PBSA, A, C and E, respectively); and mono-hydroxylated 2-phenyl-1H-benzimidazole (OH-PBI)) during photocatalytic degradation. As seen, all the intermediates quickly reached to maximum

concentration during 10–20 min followed by a gradually decay, indicating the formation and transformation of these intermediates were accompanied with the degradation of PBSA. Complete disappearance of these intermediates was observed after 90 min, suggesting TiO<sub>2</sub> photocatalysis is a promising technique for PBSA removal as well as intermediates elimination. The disappearance of the intermediates is also a reflection of further oxidation to low molecular weight organic compounds (e.g., carboxylic acids) or mineralization to inorganic ions.

### 3.4.2. Evolution of carboxylic acids

It is well-known that further oxidation of intermediates during photocatalysis usually leads to ring opening, generating a series of carboxylic acids with lower molecular weight before complete mineralization [16,31,35]. In this work, four major acids (i.e., oxalic, malonic, acetic and maleic acids) were identified by ion exchange chromatography by comparison with standards. Fig. 5B shows the evolution of these carboxylic acids as a function of irradiation time.

As seen, oxalic acid appeared as early as 30 min, and then gradually accumulated up to 57.8 μM at 210 min followed by a slow disappearance. The formation of oxalic acid can be explained either by the benzene ring opening or by dimerization of HCO<sub>2</sub> radicals as reported by previous studies [31]. Oxalic could be oxidized to two molecular of CO<sub>2</sub> by photo-holes through photo-Kolbe mechanism [16]. Since maleic acid has been known to be an important intermediate after ring opening [16], its detection in the present study was not unexpected. Malonic acid appeared at 60 min, reached a

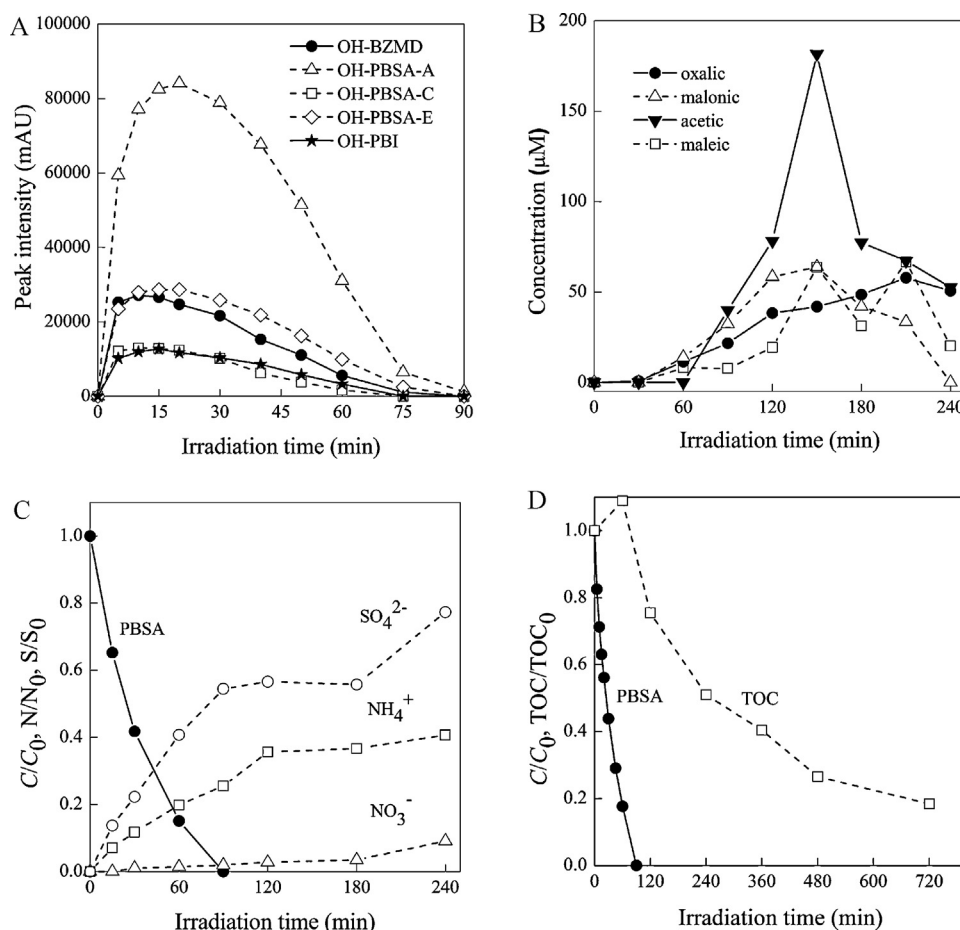


**Fig. 5.** Evolution of (A) organic intermediates, (B) carboxylic acids, (C) inorganic ions and (D) the variation of TOC during photocatalytic degradation of PBSA. Peak intensity was recorded according to HPLC–DAD spectrum. The detection wavelength was  $\lambda = 300$  nm. OH-BZMD = mono-hydroxylated benzimidine; OH-PBSA = mono-hydroxylated PBSA; OH-PBI = mono-hydroxylated 2-phenyl-1H-benzimidazole. Experimental conditions: Degussa P25 TiO<sub>2</sub> was used as photocatalyst; [TiO<sub>2</sub>] = 2.0 g L<sup>-1</sup>; [PBSA] = 45 μM; pH = 4.5.

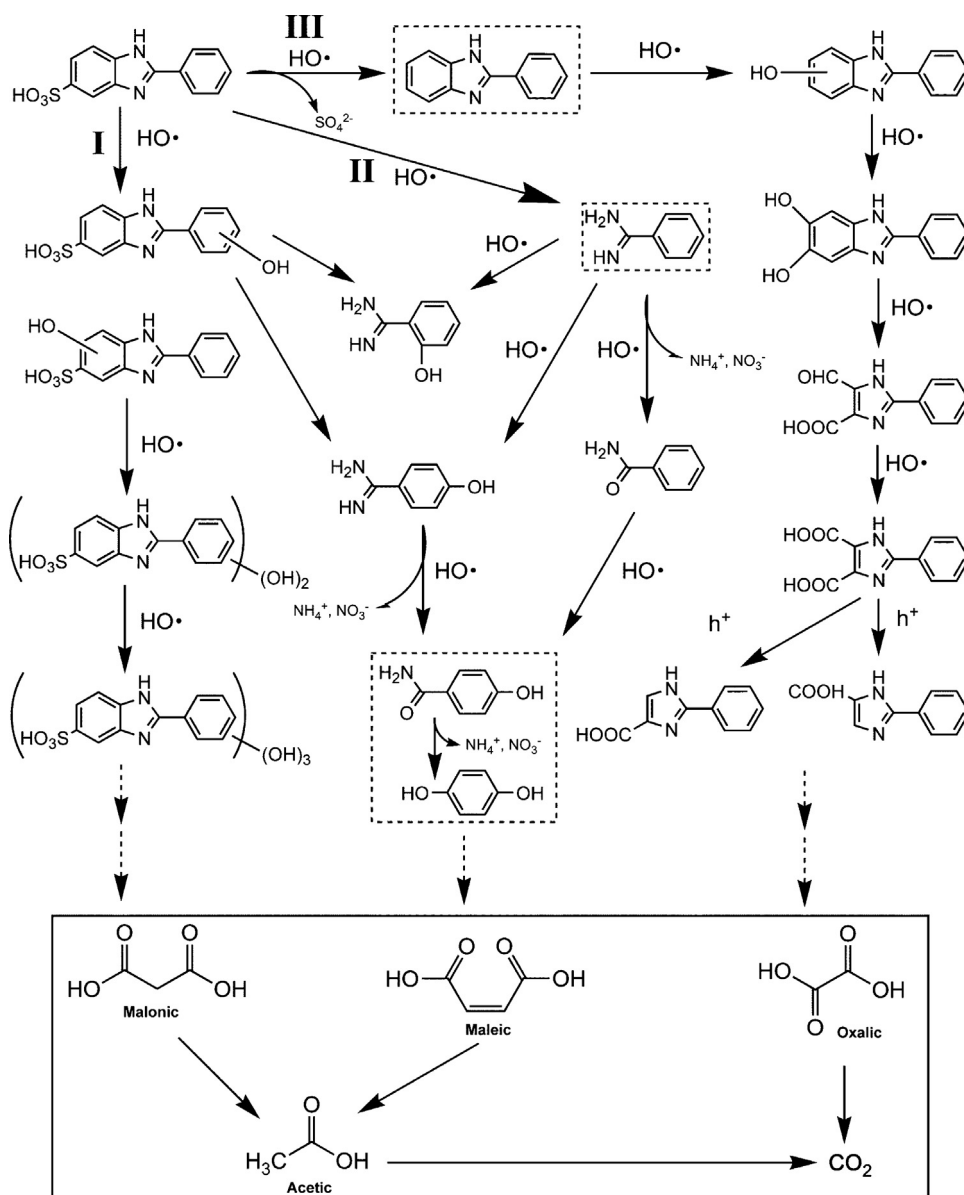


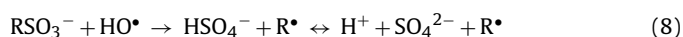
**Fig. 6.** Possible photocatalytic degradation pathways of PBSA in illuminated aqueous  $\text{TiO}_2$  suspensions. Chemicals in dash line box were not detected in this work by using LC–MS but were previously reported [14,52]. Possible formation and transformation pathways of carboxylic acids were also elucidated as proposed in solid line box.

maximum ( $63.8 \mu\text{M}$ ) at 150 min, and then gradually disappeared. Acetic acid was not observed until 90 min later and reached to maximum ( $181.6 \mu\text{M}$ ) at 150 min, followed by a notable decrease. Note that the concentration of acetic was the highest among the four carboxylic acids. Therefore, acetic acid presumably resulted from the transformation of other carboxylic acids such as malonic and maleic acids [16]. Based on the above analysis, a description of the formation and transformation of carboxylic acids is presented in solid line box in Fig. 6.

#### 3.4.3. Evolution of inorganic ions

Complete mineralization is the ultimate step in photocatalytic degradation of organic compounds. Thus, it is essential to investigate not only the disappearance of the initial pollutant but also its mineralization to  $\text{CO}_2$  and inorganic ions. The evolution of inorganic ions during PBSA photocatalysis process is depicted in Fig. 5C. As clearly seen, sulfonic moiety in PBSA was converted to sulfate ions ( $\text{SO}_4^{2-}$ ) while nitrogen atoms in imidazole structure were released as ammonium ( $\text{NH}_4^+$ ) and nitrate ( $\text{NO}_3^-$ ). At 90 min,  $45 \mu\text{M}$  PBSA

was completely degraded, while only 25.5% and 1.9% of the nitrogen and 54.5% of sulfur were released as  $\text{NH}_4^+$ ,  $\text{NO}_3^-$  and  $\text{SO}_4^{2-}$ , respectively. It is interesting to note that a majority of N was converted to  $\text{NH}_4^+$  while only a minor amount of N was transformed to  $\text{NO}_3^-$ . This observation is consistent with previous reports that nitrogen in heterocyclic aromatic rings can be transformed to both  $\text{NH}_4^+$  and  $\text{NO}_3^-$  species, while secondary, tertiary and quaternary nitrogen atoms are photo-converted predominantly to ammonium ions [45,46]. Increasing the irradiation time favors the releasing of inorganic species. At 240 min, 40.7% and 9.1% of the N and 77.3% of S were released as  $\text{NH}_4^+$ ,  $\text{NO}_3^-$  and  $\text{SO}_4^{2-}$ , respectively. It is evident that less than 50% of total N was mineralized, indicating a significant amount of nitrogenated transformation products at the end of the treatment. Therefore, 240 min irradiation seemed to be not enough to yield a full mineralization. Unlike nitrogen, sulfur is expected to be quickly converted to  $\text{SO}_4^{2-}$  under the attack of  $\text{HO}^\bullet$  as the following equation describes [47].





The reason for 77.3% S transformation ratio can be rationalized by the following: (i) complete mineralization of S containing organic intermediates was not obtained after 240 min irradiation, (ii) S atom was initially released as  $\text{HS}^-$  or  $\text{SO}_3^{2-}$  rather than directly oxidation to  $\text{SO}_4^{2-}$  [45], (iii)  $\text{SO}_4^{2-}$  was probably strongly adsorbed on  $\text{TiO}_2$  active sites which led the detection amount below the stoichiometric value [48].

#### 3.4.4. Mineralization

The photocatalytic degradation of organic pollutants usually leads to the decomposition of structure and eventually the mineralization to  $\text{CO}_2$  and  $\text{H}_2\text{O}$ , which can be visualized by the decrease of TOC [49]. Fig. 5D shows the variation of TOC during photocatalytic degradation of PBSA. It was observed that TOC reduction processed much more slowly compared to the degradation of PBSA. This finding indicates the formation of more stable intermediates toward photo-oxidation [34]. However, approximately 80% TOC was removed after 720 min irradiation. Therefore, we can expect to have a mineralization at a very long irradiation time.

#### 3.5. Elucidation of photocatalytic degradation pathways

Based on the elucidated molecular structure of photoproducts, possible  $\text{TiO}_2$ -induced photodegradation pathways of PBSA are proposed as illustrated in Fig. 6. As it can be seen, three major pathways, namely, successive hydroxylation of mother compound (Pathway I), imidazole ring cleavage (Pathway II) and de-sulfonic as well as further hydroxylation and oxidation (Pathway III), are involved in the photocatalytic degradation of PBSA.

- (I) The successive addition of  $\text{HO}^\bullet$  to mother compound leads to the formation of mono-, di-, and tri-hydroxylated PBSA. A total five mono-hydroxylation, three di-hydroxylation and one tri-hydroxylation products were detected according to LC–MS spectrum. Since  $\text{HO}^\bullet$  is known to be electrophilic, the rich electron density of benzimidazole and phenyl ring may facilitate its addition. The calculated frontier electron densities revealed that both the two benzene moiety in PBSA molecular appeared to be susceptible to the electrophilic attack of the  $\text{HO}^\bullet$ , resulting in the formation of mono-hydroxylation. It is well accepted that hydroxylation is usually the first step, but also the most important step during photocatalysis. Hydroxylated organic compounds further undergo structure decomposition, such as ring opening and chain cleavage, which eventually lead to complete mineralization [50].
- (II) The two N atoms in imidazole group have been reported to be the sites most likely attacked by  $\text{HO}^\bullet$  due to their much higher electron density [51]. The substrate molecular will break at these points, forming some precursor intermediates toward formation of  $\text{NH}_4^+$  such as an amide [52]. In this work, cleavage of the corresponding C–N bonds leads to the formation of benzamidine (BZMD). Further attack of  $\text{HO}^\bullet$  could either oxidize BZMD to benzamide or form hydroxylated benzamidine (OH-BZMD). Note that two isomers of OH-BZMD were detected according to LC–MS analysis, which possibly resulted from *para*- and *ortho*-addition because of the electron donating effect of amidine moiety. *Para*-hydroxyl benzamidine has been known to absorb appreciably at 300 nm [53], which was confirmed in our HPLC–DAD chromatogram. It is also possible that OH-BZMD arose from the C–N bonds rupture of mono-hydroxylated PBSA. BZMD has been observed previously in PBSA photolysis as an important intermediate [14]. However, it was not detected in this work, probably due to a rapid transformation under  $\text{HO}^\bullet$  attack. During  $\text{TiO}_2$  photocatalysis process,

benzamide could further transform to 4-hydroxyl benzamide and hydroquinone followed by ring opening [54].

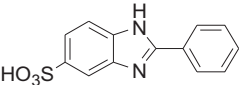
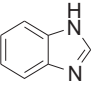
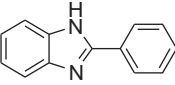
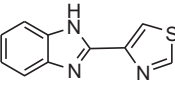
- (III) Pathway III is initiated by the detachment of sulfonic moiety in benzimidazole group, which consequently converts to sulfate. The detection of sulfate ions by ion chromatography (IC) verified the feasibility of such process. The de-sulfonic product 2-phenyl-1H-benzimidazole (PBI) further undergoes hydroxylation under the successive  $\text{HO}^\bullet$  attack. The hydroxylated PBI (OH-PBI) is supposed to generate 2-phenyl-4-carboxyl-5-aldehyde imidazole via benzene ring opening under further  $\text{HO}^\bullet$  attack. Similar benzene ring opening has been previously observed during photocatalytic degradation of thiabendazole, one kind of benzimidazole derivative fungicide which has similar structure with PBI [55]. Further oxidation of the aldehyde group generated 2-phenyl-4,5-imidazoledicarboxylic acid, which subsequently lost one carboxyl group through photo-Kolbe mechanism to form two isomers of 2-phenylimidazole carboxylic acid. It should be emphasized that some intermediate products (i.e., phenylimidazolecarboxylic derivatives and benzamide) were also observed by Zhang et al. in direct photolysis of PBSA [14], suggesting the similar degradation pathways are possibly involved in photolysis and photocatalysis.

#### 3.6. Comparison to structurally related compounds

To obtain a further insight into the mechanism of photocatalysis, PBSA was compared to benzimidazole (BI), 2-phenyl-1H-benzimidazole (PBI) and 2-(4-thiazolyl)-1H-benzimidazole (thiabendazole) in photocatalytic degradation because these compounds have a benzimidazole ring in common. Table 3 compares the experimental results of photocatalytic degradation of these benzimidazole analogs under identical conditions. PBI has the same molecular structure as PBSA except that the latter has a sulfonic moiety linking to the benzimidazole ring. Due to the electron-withdraw effect, the lack of sulfonic moiety in PBI was expected to facilitate its photocatalytic degradation via  $\text{HO}^\bullet$  attack. However, no enhancement in photocatalytic degradation rate of PBI was observed in comparison to PBSA (Table 3), suggesting 5-sulfonic moiety in PBSA had negligible effect on the photocatalysis of PBI. Previous studies have demonstrated that the two compounds actually have very similar photophysical and photochemical properties [13]. This result was also supported by the fact that the possibility of  $\text{HO}^\bullet$  attacking on 2-phenyl group is much higher than benzyl group in PBSA as illustrated by FEDs calculation. PBI has also known to be a product of PBSA upon photolysis, however, it was not detected by LC–MS in this work. BI photocatalytically degraded at a rate constant approximately 1.6 times faster than PBSA and PBI (Table 3). This result was unexpected and interesting. Due to the 2-phenyl substitution in PBSA and PBI, and the electrophilic and nonselective nature of  $\text{HO}^\bullet$ , we postulated that the photocatalytic degradation of PBSA and PBI would have processed much more rapidly than BI because 2-phenyl provided additional sites for  $\text{HO}^\bullet$  attack. However, BI was found to be more susceptible to photocatalytic destruction. It is possible that 2-phenyl substitution enabled BI molecular being more resistant to photocatalytic degradation.

A noticeable peak corresponding to the photoproduct was found in the HPLC–DAD chromatogram of the irradiated PBI sample. Although further LC–MS analysis is necessary for the accurate identification of this photoproduct, its nearly identical UV–vis spectrum relative to the mother compound as well as the early retention time implied that this photoproduct was most likely to be the hydroxylated product. This result was consistent with the Pathway III proposed in Fig. 6. A similar peak was also observed in the case of BI. The evolution of the photoproducts of PBI and BI during photocatalysis process was also depicted in Fig. S5 (Supplementary Data).

**Table 3**  
Photocatalytic degradation of PBSA and structurally related compounds.

Compounds	Molecular structure	Degradation rate constant ( $\text{min}^{-1}$ ) <sup>a</sup>	Linear correlation coefficient ( $R^2$ )
2-Phenylbenzimidazole-5-sulfonic acid (PBSA)		$0.0381 \pm 0.0026$	0.999
Benzimidazole (BI)		$0.0591 \pm 0.0064$	0.980
2-Phenyl-1H-benzimidazole (PBI)		$0.0352 \pm 0.0022$	0.996–0.999
2-(4-thiazolyl)-1H-Benzimidazole (thiabendazole) <sup>b</sup>		NA <sup>c</sup>	NA

<sup>a</sup> Experimental conditions: Degussa P25  $\text{TiO}_2$  was used as photocatalyst; [substrate] = 45  $\mu\text{M}$ ;  $[\text{TiO}_2]$  = 1.0  $\text{g L}^{-1}$ ; pH = 7.0. Errors are 95% confidence intervals.

<sup>b</sup> Photocatalytic degradation pathways of thiabendazole was compared to PBSA according to Ref. [55].

<sup>c</sup> NA = not available. No kinetic data of thiabendazole photocatalysis was available in Ref. [55].

Note that the evolution profiles were only qualitative because there were no standards available of the photoproducts to ensure their quantitative analysis.

On the other hand, thiabendazole, a widely used fungicide, has a thiazole ring adjacent to benzimidazole ring instead of a phenyl ring in PBI. A previous study on identification of thiabendazole phototransformation products on  $\text{TiO}_2$  by Calza et al. showed that there are two different parallel pathways: (i) the hydroxylation of the molecular on the aromatic ring, a further oxidation leads to ring opening and to the formation of aldehydic and alcoholic structure; (ii) the cleavage of a C–C bond and the formation of benzimidazole [55]. It is apparent that Pathway I was identical to the Pathway III as we proposed in photocatalytic degradation of PBSA in this work (Fig. 6). However, the cleavage of the bond between benzimidazole and phenyl ring was not observed in the present study, which differed from thiabendazole in photocatalytic degradation. This finding can be explained by the strong  $\pi$ – $\pi$  conjugation of benzimidazole and phenyl ring, resulting in the bond being stable. Similar result has been observed previously by a study on photolysis of various 2-substituted benzimidazoles [56]. It has been proposed that 2-phenyl group stabilizes the benzimidazole ring system to photolysis as does the 2-thiazolyl group; however, the latter suffers thiazole ring cleavage [56]. This finding also supported the above result that BI was substantially more susceptible to photocatalytic degradation compared to PBSA and PBI.

#### 4. Conclusions

The aqueous photocatalytic degradation of sunscreen agent 2-phenylbenzimidazole-5-sulfonic acid (PBSA) has been studied in illuminated  $\text{TiO}_2$  suspensions.  $\text{TiO}_2$ -induced photocatalysis resulted in a pronounced degradation of PBSA. Photocatalytic reactions followed pseudo-first-order kinetics. Radical scavenger experiments indicated that  $\text{HO}^\bullet$  was the predominant radical responsible for an appreciable degradation of PBSA. Second-order rate constant of PBSA- $\text{HO}^\bullet$  reaction was determined to be  $5.8 \times 10^9 \text{ M}^{-1} \text{ s}^{-1}$  by competition kinetics method, suggesting  $\text{HO}^\bullet$ -mediated PBSA oxidation is near the diffusion-controlled limit. Organic intermediates were identified by LC–MS analysis, and the major photoproducts included hydroxylated products, imidazole ring cleavage compounds and phenylimidazolecarboxylic derivatives. Frontier electron densities (FEDs) calculation predicted that

both the two benzenes in PBSA are likely to be attacked by  $\text{HO}^\bullet$ , resulting in the formation of mono-hydroxylation products. Four carboxylic acids, oxalic, malonic, acetic and maleic acids were detected during PBSA photocatalysis. Sulfonic moiety of PBSA was primarily released as a sulfate ion while nitrogen atoms were converted predominantly to ammonium and a less extent to nitrate. Approximately 80% TOC was removed after 720 min irradiation, implying mineralization can be expected to obtain after a very long irradiation time. A comparative study on photocatalytic degradation of PBSA and structurally related compounds revealed that the 5-sulfonic moiety had negligible effect on the photocatalysis while 2-phenyl substituent stabilized the benzimidazole ring system to photocatalytic degradation.

Although results from the present study suggest that  $\text{TiO}_2$  photocatalysis is a promising treatment technology for sunscreen agent PBSA, a thorough evaluation of the toxicity of intermediates is essential in order to optimize photocatalytic treatment and evaluate the potential risks to the ecology system before the technology is applied for water purification.

#### Acknowledgements

This work was supported by National Natural Science Foundation of China (Nos. 20977045 and 21177056) and Fundamental Research Funds for the Central Universities (1112021101) and Yue-fei Ji gratefully acknowledges the China Scholarship Council (CSC) for the financial support. The authors also would like to thank the scientific services of Institut de recherches sur la catalyse et l'environnement de Lyon (IRCELYON).

#### Appendix A. Supplementary data

Supplementary data associated with this article can be found, in the online version, at <http://dx.doi.org/10.1016/j.apcatb.2013.04.046>.

#### References

- [1] F.P. Gasparro, *Environmental Health Perspectives* 108 (2000) 71–78.
- [2] T. Poiger, H.R. Buser, M.E. Balmer, P.A. Bergqvist, M.D. Müller, *Chemosphere* 55 (2004) 951–963.
- [3] C. Plagellat, T. Kupper, R. Furrer, L.F. de Alencastro, D. Grandjean, J. Tarradellas, *Chemosphere* 62 (2006) 915–925.

- [4] P. Gago-Ferrero, M. Silvia Díaz-Cruz, D. Barceló, *Analytical Methods* 5 (2013) 355–366.
- [5] R.P. Schwarzenbach, B.I. Escher, K. Fenner, T.B. Hofstetter, C. Annette Johnson, U. von Gunten, B. Wehrli, *Science* 313 (2006) 1072–1077.
- [6] M. Schlumpf, P. Schmid, S. Durrer, M. Conscience, K. Maerkel, M. Henseler, M. Gruetter, I. Herzog, S. Reolon, R. Ceccatelli, O. Faass, E. Stutz, H. Jarry, W. Wuttke, W. Lichtensteiger, *Toxicology* 205 (2004) 113–122.
- [7] M. Silvia Díaz-Cruz, D. Barceló, *Trends in Analytical Chemistry* 28 (2009) 708–716.
- [8] M. Silvia Díaz-Cruz, M. Llorca, D. Barceló, *Trends in Analytical Chemistry* 27 (2008) 873–887.
- [9] C.G. Daughton, T.A. Ternes, *Environmental Health Perspectives* 107 (1999) 907–938.
- [10] R. Rodil, J.B. Quintana, P. López-Mahía, S. Muniategui-Lorenzo, D. Prada-Rodríguez, *Analytical Chemistry* 80 (2008) 1307–1315.
- [11] E. Gilbert, F. Pirot, V. Bertholle, L. Roussel, F. Falson, K. Padois, *International Journal of Cosmetic Science* (2013), <http://dx.doi.org/10.1111/ics.12030>.
- [12] M. Krause, A. Klit, M. Blomberg Jensen, T. Søborg, H. Frederiksen, M. Schlumpf, W. Lichtensteiger, N.E. Skakkebaek, K.T. Drzewiecki, *International Journal of Andrology* 35 (2012) 424–436.
- [13] J. Johnson Inbaraj, P. Bilski, C.F. Chignell, *Photochemistry and Photobiology* 75 (2002) 107–116.
- [14] S. Zhang, J. Chen, X. Qiao, L. Ge, X. Cai, G. Na, *Environmental Science and Technology* 44 (2010) 7484–7490.
- [15] S. Zhang, J. Chen, Y. Wang, X. Wei, *Environmental Chemistry Letters* 10 (2012) 389–394.
- [16] J.-M. Herrmann, *Catalysis Today* 53 (1999) 115–129.
- [17] M. Nan Chong, B. Jin, C.W.K. Chow, C. Saint, *Water Research* 44 (2010) 2997–3027.
- [18] Y. Chen, C. Hu, X. Hu, J. Qu, *Environmental Science and Technology* 43 (2009) 2760–2765.
- [19] A.A. Khodja, B. Lavedrine, C. Richard, T. Sehili, *International Journal of Photoenergy* 4 (2002) 147–151.
- [20] M.M. Haque, M. Muneer, D.W. Bahnemann, *Environmental Science and Technology* 40 (2006) 4765–4770.
- [21] D.C. Hurum, A.G. Agrios, K.A. Gray, *Journal of Physical Chemistry B* 107 (2003) 4545–4549.
- [22] J. Ryu, W. Choi, *Environmental Science and Technology* 42 (2008) 294–300.
- [23] Y.F. Rao, W. Chu, *Environmental Science and Technology* 43 (2009) 6183–6189.
- [24] J. Kim, C.W. Lee, W. Choi, *Environmental Science and Technology* 44 (2010) 6849–6854.
- [25] H. Park, Y. Park, W. Kim, W. Choi, *Journal of Photochemistry and Photobiology C: Photochemistry Review* (2012), <http://dx.doi.org/10.1016/j.jphotochemrev.2012.10.001>.
- [26] Y. Sun, J.J. Pignatello, *Environmental Science and Technology* 29 (1995) 2065–2072.
- [27] Y. Chen, S. Yang, K. Wang, L. Lou, *Journal of Photochemistry and Photobiology A: Chemistry* 172 (2005) 47–54.
- [28] S.T. Martin, A.T. Lee, M.R. Hoffmann, *Environmental Science and Technology* 29 (1995) 2567–2573.
- [29] L. Yang, L.E. Yu, M.B. Ray, *Environmental Science and Technology* 43 (2009) 460–465.
- [30] E. Hapeshi, A. Achilleos, M.I. Vasquez, C. Michael, N.P. Xekoukoulotakis, D. Mantzavinos, D. Kassinos, *Water Research* 44 (2010) 1737–1746.
- [31] M. Sleiman, P. Conchon, C. Ferronato, J.-M. Chovelon, *Applied Catalysis B: Environmental* 71 (2007) 279–290.
- [32] S. Ahmed, M.G. Rasul, R. Brown, M.A. Hashib, *Journal of Environment Management* 92 (2011) 311–330.
- [33] B. Abramović, D. Šojić, V. Despotović, D. Vione, M. Pazzi, J. Csanádi, *Applied Catalysis B: Environmental* 105 (2011) 191–198.
- [34] X. Lin, C. Ferronato, N. Deng, F. Wu, J.-M. Chovelon, *Applied Catalysis B: Environmental* 88 (2009) 32–41.
- [35] L. Lagunas-Allué, M.-T. Martínez-Soria, J. Sanz-Asensio, A. Salvador, C. Ferronato, J.-M. Chovelon, *Applied Catalysis B: Environmental* 98 (2010) 122–131.
- [36] J. Radjenović, C. Sirtori, M. Petrović, D. Barceló, S. Malato, *Applied Catalysis B: Environmental* 89 (2009) 255–264.
- [37] C. Sirtori, A. Agüera, W. Gernjak, S. Malato, *Water Research* 44 (2010) 2735–2744.
- [38] J.P. Huang, S.A. Mabury, *Environmental Toxicology and Chemistry* 19 (2000) 2181–2188.
- [39] P.L. Brezonik, J. Fulkerson-Brekken, *Environmental Science and Technology* 32 (1998) 3004–3010.
- [40] L. Hu, P.M. Flanders, P.L. Miller, T.J. Strathmann, *Water Research* 41 (2007) 2612–2626.
- [41] N. Corin, P. Backlund, M. Kulovaara, *Chemosphere* 33 (1996) 245–255.
- [42] K. Fukui, T. Yonezawa, H. Shingu, *Journal of Chemical Physics* 20 (1952) 722–725.
- [43] K. Fukui, T. Yonezawa, T. Nagata, *Journal of Chemical Physics* 22 (1954) 1433–1442.
- [44] Y. Ohko, K. Iuchi, C. Niwa, T. Tatsuma, T. Nakashima, T. Iguchi, Y. Kubota, A. Fujishima, *Environmental Science and Technology* 36 (2002) 4175–4181.
- [45] P. Calza, C. Medana, C. Baiocchi, E. Pelizzetti, *Journal of Photochemistry and Photobiology A: Chemistry* 189 (2007) 380–386.
- [46] H. Yang, G. Li, T. An, Y. Gao, J. Fu, *Catalysis Today* 153 (2010) 200–207.
- [47] E. Szabó-Bárdos, O. Markovics, O. Horváth, N. Törő, G. Kiss, *Water Research* 45 (2011) 1617–1628.
- [48] M. Sleiman, D. Vildoza, C. Ferronato, J.-M. Chovelon, *Applied Catalysis B: Environmental* 77 (2007) 1–11.
- [49] L. Lagunas-Allué, M.-T. Martínez-Soria, J. Sanz-Asensio, A. Salvador, C. Ferronato, J.-M. Chovelon, *Applied Catalysis B: Environmental* 115–116 (2012) 285–293.
- [50] F. Méndez-Arriaga, S. Esplugas, J. Giménez, *Water Research* 42 (2008) 585–594.
- [51] H. Hidaka, E. García-López, L. Palmisano, N. Serpone, *Applied Catalysis B: Environmental* 78 (2008) 139–150.
- [52] E. Pelizzetti, P. Calza, G. Mariella, V. Maurino, C. Minero, H. Hidaka, *Chemical Communications* 13 (2004) 1504–1505.
- [53] E. Rogana, D.L. Nelson, M. Mares-Guia, *Journal of the American Chemical Society* 97 (1975) 6844–6848.
- [54] A. Piscopo, D. Robert, J.V. Weber, *Journal of Photochemistry and Photobiology A: Chemistry* 139 (2001) 253–256.
- [55] P. Calza, S. Baudino, R. Aigotti, C. Baiocchi, E. Pelizzetti, *Journal of Chromatography A* 984 (2003) 59–66.
- [56] G. Crank, A. Mursyidi, *Australian Journal of Chemistry* 35 (1982) 775–784.